research articles Journal of proteome research

Global Metabolic Responses of NMRI Mice to an Experimental *Plasmodium berghei* Infection

Jia V. Li,[†,‡] Yulan Wang,[†,#] Jasmina Saric,[†,‡] Jeremy K. Nicholson,[†] Stephan Dirnhofer,[§] Burton H. Singer,[||] Marcel Tanner,[‡] Sergio Wittlin,[⊥] Elaine Holmes,[†] and Jürg Utzinger*[,‡]

Department of Biomolecular Medicine, Division of Surgery, Oncology, Reproductive Biology and Anaesthetics (SORA), Faculty of Medicine, Imperial College London, Sir Alexander Fleming Building, South Kensington, London SW7 2AZ, United Kingdom, Department of Public Health and Epidemiology, Swiss Tropical Institute, P.O. Box, CH-4002 Basel, Switzerland, Institute of Pathology, University Hospital Basel, Schönbeinstrasse 40, CH-4031 Basel, Switzerland, Office of Population Research, Princeton University, Wallace Hall 245, Princeton, New Jersey 08544, and Department of Medical Parasitology and Infection Biology, Swiss Tropical Institute, P.O. Box, CH-4002 Basel, Switzerland

Received March 20, 2008

We present a metabolism-driven top-down systems biology approach to characterize metabolic changes in the mouse resulting from an infection with *Plasmodium berghei*, using high-resolution ^{1}H NMR spectroscopy and multivariate data analysis techniques. Twelve female NMRI mice were infected intravenously with ~20 million *P. berghei*-parasitized erythrocytes. Urine and plasma samples were collected 4−6 h before infection, and at days 1, 2, 3, and 4 postinfection. Multivariate analysis of spectral data showed differentiation between samples collected before and after infection, with growing metabolic distinction as the time postinfection progressed. Our analysis of plasma from *P. berghei*-infected mice showed marked increases in lactate and pyruvate levels, and decreased glucose, creatine, and glycerophosphoryl choline compared with preinfection, indicating glycolytic upregulation, and increased energy demand due to *P. berghei* infection. The dominant changes in the urinary metabolite profiles included increased levels of pipecolic acid, phenylacetylglycine, and dimethylamine, and decreased concentrations of taurine and trimethylamine-*N*-oxide, which may, among other factors, indicate a disturbance of the gut microbial community caused by the parasite. Although several of the observed metabolic changes are also associated with other parasitic infections, the combination of metabolic changes and, in particular, the occurrence of pipecolic acid in mouse urine postinfection are unique to a *P. berghei* infection. Hence, metabolic profiling may provide a sensitive diagnostic tool of *Plasmodium* infection and the control of malaria more generally.

Keywords: malaria • *Plasmodium berghei* • mouse • metabonomics • metabolomics • ^{1}H NMR spectroscopy • multivariate data analysis • urine • plasma

Introduction

Malaria, which is caused by an infection of a protozoan of the genus *Plasmodium*, is the most severe and widespread parasitic disease in the tropics and subtropics. Indeed, malaria due to *Plasmodium falciparum* accounted for >500 million clinical disease episodes in 2002,[1] and >1 million deaths were attributed to the disease in 2001.[2] Malaria is particularly rampant in sub-Saharan Africa, with children under the age of 5 years and pregnant women at highest risk of disease-associated morbidity and mortality.[3,4] The global burden of malaria is currently estimated at ~40 million disability-adjusted life years (DALYs).[2] Among more than 100 species of *Plasmodium*, four infect humans, that is, *P. falciparum*, *Plasmodium malariae*, *Plasmodium ovale*, and *Plasmodium vivax*.[4] The molecular mechanisms of infection and response to therapeutic interventions have been studied extensively in rodent models using murine malaria parasites, including *Plasmodium berghei*, *Plasmodium chabaudi*, *Plasmodium vinckei*, and *Plasmodium yoelii*.[5−8]

There is a new global emphasis on the eradication of malaria, but the challenges ahead to control, let alone local elimination or eradication of the disease, are formidable.[9] A particularly vexing problem is the large number of asymptomatic carriers[10,11] for whom detection of parasitemia with conventional methods is difficult. Hence, there is a need to discover, develop, and

* To whom correspondence should be addressed. Jürg Utzinger, Department of Public Health and Epidemiology, Swiss Tropical Institute, P.O. Box, CH-4002 Basel, Switzerland. Tel, +41 61 284-8129; fax, +41 61 284-8105. E-mail: juerg.utzinger@unibas.ch.
† Imperial College London.
‡ Department of Public Health and Epidemiology, Swiss Tropical Institute.
# Present address: State Key Laboratory of Magnetic Resonance and Atomic and Molecular Physics, Wuhan Institute of Physics and Mathematics, Chinese Academy of Sciences, Wuhan 430071, People's Republic of China.
§ University Hospital Basel.
|| Princeton University.
⊥ Department of Medical Parasitology and Infection Biology, Swiss Tropical Institute.

10.1021/pr800209d CCC: $40.75
Published on Web 07/23/2008

deploy novel tools and strategies for biomarker discovery to aid diagnosis, interventions and integrated control packages. Access to prompt diagnosis and efficacious antimalarial drugs, for example, is one of the current pillars of malaria control. Microscopic detection of parasites in finger prick blood samples remains the most widely used diagnostic test in malaria-endemic settings. This approach allows determination of the degree of infection (parasitemia) at relatively low cost, but requires experienced microscopists, and lacks sensitivity at low levels of parasitemia. A number of rapid malaria diagnostic tests have been developed over the past decade. They are based on immunochromatographic dipstick assays and find increasing use for self-diagnosis, but are costly and have imperfect sensitivity, particularly when parasitemia is low.[12] The issue of diagnosis is just one example to illustrate the need for new and improved tools that can be utilized for individual diagnosis of malaria and for monitoring disease control programs and, hence, measuring progress toward local elimination and eradication. Various technological approaches, including transcriptomics, have been utilized to characterize malaria infection and to further our understanding of the difference between parasite strains.[13]

The combination of high-resolution ^{1}H NMR spectroscopy of biofluids and tissue samples with multivariate statistical analysis has been shown to be useful in biomarker discovery and, hence, may facilitate development of new diagnostic tools, drug targets, and vaccines.[14–16] Here, we explore further the characteristics of malarial infection by applying a metabolism-driven top-down systems biology strategy that has proved effective in studying transgenomic interactions in mammalian symbiotic systems, for example, the gut microbiota.[17,18] Similar approaches have also been successfully applied to characterize the systemic metabolic fingerprints of *Schistosoma* spp. and *Trypanosoma* spp. infections in rodent models.[19–21] To establish the metabolic consequences of a *P. berghei* infection, we focus on a mouse model and compare urinary and plasma metabolite profiles from host animals prior to infection with profiles generated from biofluids obtained 1−4 days postinfection. The ultimate goal is to enhance our understanding of the metabolic response to a *Plasmodium* infection and to identify candidate biomarkers that may be translatable to diagnosis and prognosis in human populations. Our investigation is complemented with a histological examination of kidney, liver, and spleen obtained from *P. berghei*-infected mice upon dissection, that is, at day 4 postinfection.

Materials and Methods

***P. berghei*-Mouse Model.** The animal experiments described here were carried out at the Swiss Tropical Institute (Basel, Switzerland), adhering to local and national regulations of laboratory animal welfare in Switzerland (permission no. 2081). A total of 12 out-bred NMRI strain female mice, aged ∼3 weeks, were purchased from RCC (Füllinsdorf, Switzerland) and acclimatized for 4 days. Mice were randomly allocated to 1 of 3 cages, marked with individual identifiers, and group-housed in batches of 4 throughout the study. Mice were kept in stable environmental conditions (temperature, 22 °C; relative humidity, 60−70%; 12-h light/12-h dark cycle) and had free access to community tap water and special pellet diet (9009 PAB-45, purchased from Provimi Kliba AG; Kaiseraugst, Switzerland). At the onset of the experiment, mice weighed between 22.7 and 26.5 g (mean = 23.8 g; standard deviation (SD) = 1.2 g).

Each mouse was infected intravenously with ∼20 million parasitized erythrocytes (GFP-transfected *P. berghei* strain ANKA[22]), as follows: heparinized blood from a donor mouse with ∼30% parasitemia was taken, diluted in physiological saline to ∼100 million parasitized erythrocytes per mL of blood, and an aliquot of 0.2 mL of this suspension (containing ∼20 million *P. berghei*-parasitized erythrocytes) was then used for injection.[23]

Biofluid Collection. Samples of urine and blood were collected at 5 time points, that is, 4−6 h before infection, and at days 1, 2, 3, and 4 postinfection. Following sample collection, the body weights of mice were measured using a Mettler balance (model K7T; Greifensee, Switzerland).

Sample collection was always carried out between 08:00 and 11:00 to minimize diurnal variations in urinary and plasma metabolite concentrations. At least 20 μL of urine was collected into a Petri dish by gently rubbing the abdomen of the mouse. Mice that failed to generate sufficient quantities of urine were placed individually into empty cages and observed until they released a few drops of urine which was immediately collected with a micropipette. Urine was transferred into 1.5 mL Eppendorf tubes, placed on dry ice, and transferred to a freezer at −80 °C.

Between 40 and 50 μL of blood was collected into a Sodium-heparin hematocrit capillary (Brand GMBH + CO KG; Wertheim, Germany) from the tail of the mouse by cutting off its tip. Subsequently, plasma was separated from red blood cells by centrifugation (model 1−15, Sigma; Osterode am Harz, Germany) at 4000*g* for 5 min. The ratio of plasma to red blood cells was measured and the packed cell volume (PCV) determined and expressed as a percentage. The plasma was then transferred into a 1.5 mL Eppendorf tube, placed on dry ice, and transferred to a freezer at −80 °C. Parasitemia was determined with a FACScan (Becton Dickinson; Basel, Switzerland) by counting 100 000 red blood cells, as previously described.[22]

Histology. On day 4 postinfection, after the final sampling of biofluids, mice were killed using the standard CO_2 method. The right kidney and small portions of the liver and spleen were removed and transferred in Eppendorf tubes containing 10% formalin. Sections of these organs were cut and stained with hematoxylin and eosin prior to examination under a microscope. The results were compared with those obtained from a satellite group of noninfected control mice of the same age and sex, maintained under the same environmental conditions and killed at the same time point.

Sample Preparation and ^{1}H NMR Spectroscopic Analysis. Urine and plasma samples were forwarded on dry ice to Imperial College (London, U.K.) for subsequent ^{1}H NMR analyses. Individual urine samples (20 μL) were mixed with equal amounts of phosphate buffer (D_2O/H_2O (v/v), 1:1; pH 7.4), containing sodium 3-(trimethylsilyl) propionate-2,2,3,3-d_4 (TSP, 0.05%) for a chemical shift reference, and 3 mM Na azide was transferred into a 1.7 mm micro-NMR tube. A standard one-dimensional (1D) ^{1}H NMR spectrum was acquired for each urine sample with a pulse (recycle delay (RD)-90°-t_1-90°-t_m-90°-acquire free induction decay (FID)) on a Bruker DRX 600 MHz spectrometer (Rheinstetten, Germany), using a 5 mm triple resonance with inversion detection (TXI) probe operating at 600.13 MHz. The field frequency was locked on D_2O solvent. The water peak was suppressed by irradiation during the RD of 2 s and mixing time (t_m) of 100 ms. The t_1 was fixed to 3 μs. The 90° pulse length was adjusted to ∼10 μs.

Table 1. Mean PCV, Parasitemia and Body Weight in a Group of 12 Female NMRI Mice Before and at Different Time Points after Inoculation with ~20 Million *P. berghei*-Infected Erythrocytes

	mean (SD)		
time point	PCV in %[a]	parasitemia in %	body weight in g
4−6 h preinfection	55 (4)	-	23.8 (1.2)
day 1 postinfection	49 (3)*	0.4 (0.1)	23.5 (1.5)
day 2 postinfection	47 (4)*	4.1 (0.2)	23.9 (1.6)
day 3 postinfection	44 (4)*	16.3 (2.0)	23.9 (1.7)
day 4 postinfection	33 (3)*	34.4 (5.2)	23.9 (1.6)

[a] Asterisk (*) indicates $p < 0.001$.

For each sample, 64 scans were recorded into ~32 000 data points with a spectral width of 20 ppm. An exponential line broadening function of 0.3 Hz was applied to FID prior to Fourier transformation. Additionally, two-dimensional (2D) NMR experiments, using ^{1}H−^{1}H correlation spectroscopy (COSY) and total correlation spectroscopy (TOCSY) to assist metabolite identification, were also carried out on selected urine samples utilizing standard acquisition parameters.[19] A total of 128 increments with 80 scans were accumulated into 2000 data points with a spectral width of 10 ppm for each dimension.

Individual plasma samples were prepared by mixing 20 μL of plasma with an equal amount of saline (D_2O/H_2O (v/v), 1:1, 0.9% NaCl). Subsequently, this mixture was placed into 1.7 mm micro-NMR tubes. A 1D ^{1}H NMR experiment with Carr-Purcell-Meiboom-Gill (CPMG) pulse (RD-90°-(τ-180°-τ)$_n$-acquire FID) was acquired for each sample using a spectral width of 20 ppm and 256 transients collected into ~32 000 data points. Water suppression was achieved as described previously for urine samples.

Data Reduction and Multivariate Analysis. ^{1}H NMR spectra obtained from urine and plasma were automatically phased and baseline-corrected, using an in-house developed MATLAB script (T. Ebbels, Imperial College London). Urine spectra were referenced to the TSP resonance at δ 0.00, whereas plasma spectra were referenced to the anomeric proton signal from α-glucose at δ 5.23. The complete spectra (δ 0.0−10.0) were each digitized into ~40 000 data points using another in-house developed MATLAB script (O. Cloarec, Imperial College London). The regions between δ 4.20 and δ 6.24 in urine spectra, and between δ 4.50 and δ 5.10 in plasma spectra were removed in order to minimize the effect of the baseline distortion caused by imperfect water suppression. Additionally, the regions δ 0.0−0.85 and δ 8.5−10.0 in urine spectra, and the regions δ 0.0−0.8 and δ 8.5−10.0 in plasma spectra containing only noise were also removed.

For each spectrum, normalization to the entire remaining spectrum was performed before multivariate data analysis was carried out. A supervised multivariate data analysis tool, orthogonal-projection to latent structure-discriminant analysis (O-PLS-DA),[24] was applied to the analysis of ^{1}H NMR spectral data scaled to unit variance in a MATLAB environment, using in-house developed scripts. This method employed back-scaled transformation of the variables to the covariance matrix in order to facilitate interpretation of the results.

Results

***P. berghei* Infection and Histological Observations.** Table 1 shows the mean PCV, parasitemia and body weight in a group of 12 female NMRI mice 4−6 h before, and at days 1, 2, 3, and 4 after animals were inoculated with ~20 million *P. berghei*-infected erythrocytes each. The mean PCV dropped from 55% preinfection to 33% by the end of experiment. Using a *t*-test allowing for unequal variance revealed that the difference between the mean PCV values preinfection and postinfection was highly significant, already at day 1 postinfection ($p < 0.001$). Parasitemia increased exponentially from day 1 to day 4 postinfection, reaching a mean value of 34.4% at the final observation 4 days postinfection. The mean body weight of the group of mice stayed constant over the 4-day period of the experiment.

Histological examination of the spleen obtained from *P. berghei*-infected mice on termination of the experiment (i.e., day 4 postinfection) showed signs of a response to a systemic infection. In particular, there was an impressive reactive follicular hyperplasia of white pulp nodules that was accompanied by red pulp congestion with abundant hemozoin in cordal macrophages in all infected animals (Figure 1). Cellular architecture in both liver and kidney appeared normal, although there was a tendency of a higher quantity of tubular cell damage in the kidney.

^{1}H NMR Spectroscopy of Mouse Urine. Typical ^{1}H NMR spectra of urine obtained from mice 4−6 h preinfection, and 4 days after infection with *P. berghei* are shown in Figure 2, panels A and B, respectively. Metabolite identification was assisted by our in-house database, coupled with 2D COSY and TOCSY (results not shown). Metabolites identified from urine of both pre- and postinfected mice included 2-oxoisovalerate, 3-methyl-2-oxovalerate, 3-carboxy-2-methyl-3-oxopropanamine, acetate, citrate, succinate, dimethylamine, trimethylamine, 2-oxoglutarate, creatine, creatinine, trimethylamine-*N*-oxide (TMAO), taurine, phenylacetylglycine (PAG), 2-oxoisocaproate, 3-ureidopropanoic acid, lactate, pyruvate, *p*-cresol-glucuronide, and formate, as shown in Figure 2. Additionally, pipecolic acid was found, however, only in urine samples obtained from mice after infection with *P. berghei*. In order to focus on the metabolite changes with infection, we systematically employed an O-PLS-DA strategy.[24]

Multivariate Analysis of ^{1}H NMR Spectra of Urine. The O-PLS-DA models comparing pre- and postinfection spectral data were built using NMR data as the *X*-matrix and class information (i.e., pre- or postinfection) as the *Y*-matrix. For each sample collection time, a model was constructed in which one PLS component and one orthogonal component was calculated, using spectral data scaled to unit variance (Figure 3). The color of the variables or signals in the O-PLS-DA coefficient plots indicates significance of metabolites contributing to group separation, that is, between pre- and postinfection time points. The significance level increases from blue (no correlation with class) to red (highly significant in discriminating between classes), which is shown in the color bar on the right-hand side of the O-PLS-DA coefficient plots. The orienta-

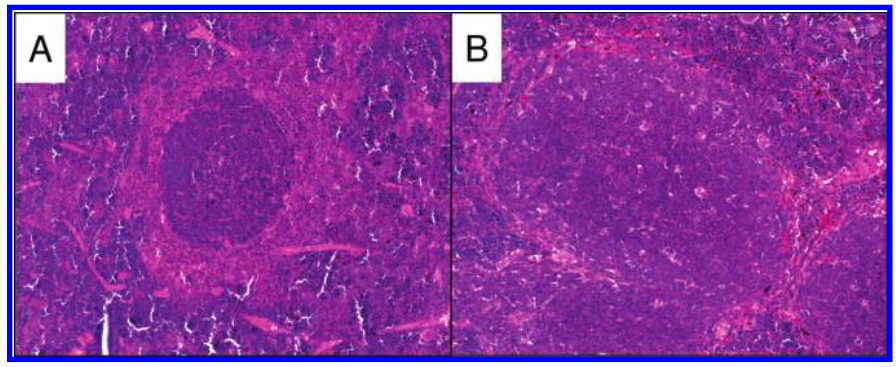

Figure 1. Section of a spleen obtained from a *P. berghei*-infected mouse 4 days postinfection showing a marked reactive follicular hyperplasia with large, nearly confluent germinal centers consisting of centroblasts and immunoblasts. In addition, there was red pulp congestion with abundant hemozoin in cordal macrophages (A). For comparison, a section of a spleen from a healthy control mouse (same strain, age- and sex-matched) is also shown. Note the small nonstimulated primary follicle and the lack of malarial hemozoin pigment (B).

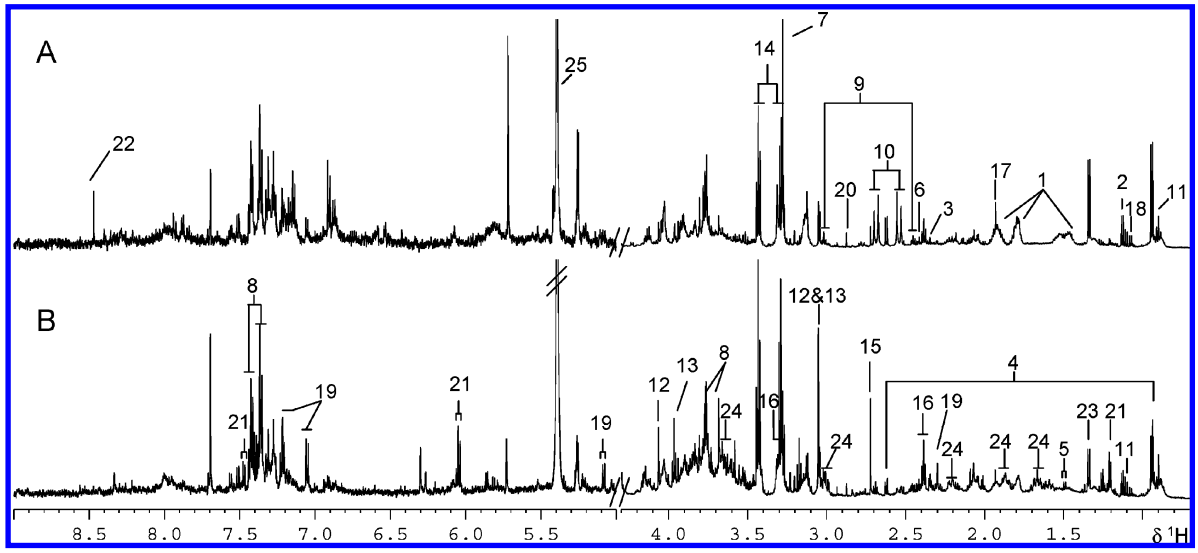

Figure 2. Typical 600 MHz ^{1}H NMR spectra of urine obtained from a preinfected mouse (A) and a mouse 4 days after a *P. berghei* infection (B). Keys: 1, lysine; 2, 2-oxoisovalerate; 3, pyruvate; 4, 2-oxoisocaproate; 5, alanine; 6, succinate; 7, trimethylamine-*N*-oxide (TMAO); 8, phenylacetylglycine (PAG); 9, 2-oxoglutarate; 10, citrate; 11, 3-methyl-2-oxovalerate; 12, creatinine; 13, creatine; 14, taurine; 15, dimethylamine; 16, 3-ureidopropanoic acid; 17, acetate; 18, 3-carboxy-2-methyl-3-oxopropanamine; 19, *p*-cresol-glucuronide; 20, trimethylamine; 21, cytosine; 22, formate; 23, lactate; 24, pipecolic acid; 25, allantoin; 26, alanine.

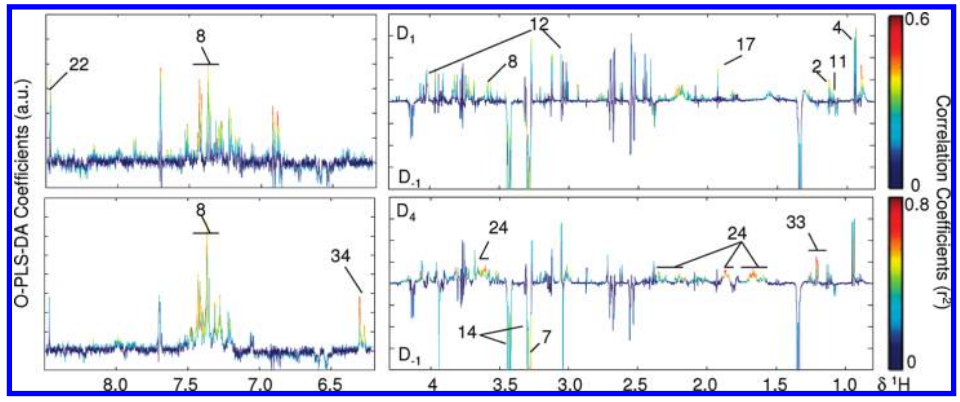

Figure 3. O-PLS coefficient plots derived from ^{1}H NMR spectra of urine individually collected from mice prior to a *P. berghei* infection and daily postinfection, illustrating the metabolic discrimination between the pre- and postinfection stages. The respective Q^2Y values for days 1 and 4 postinfection were 0.25 and 0.57 in those two O-PLS coefficient plots.

tion of peaks in the plot describes the trend of changes of metabolites; upward orientation reflecting a relatively increased level of metabolite postinfection in comparison to the preinfection time point and *vice versa*.

The main metabolites contributing to the differentiation between NMR spectral data obtained from mouse urine before and after mice were infected with *P. berghei* are summarized in Table 2. In addition, goodness of fit (expressed as R^2X) and

Table 2. Changes of Metabolites Observed in Urine Obtained from Mice at Different Time Points after Infection with *P. berghei*, Compared with Preinfection Time Point

		importance of contribution at different time points postinfection			
metabolite (key[a])	chemical shift (δ^1H)	day 1 ($Q^2Y = 0.25$; $R^2X = 0.27$)	day 2 ($Q^2Y = 0.23$; $R^2X = 0.22$)	day 3 ($Q^2Y = 0.45$; $R^2X = 0.31$)	day 4 ($Q^2Y = 0.57$; $R^2X = 0.35$)
2-oxoisocaproate (4)	0.93(d), 2.09(m), 2.62(d)	+0.57	-	-	-
2-oxoisovalerate (2)	1.13(d), 3.02(m)	+0.68	-	-	-
3-methyl-2-oxovalerate (11)	0.90(t), 1.10(d)	+0.67	-	-	-
creatinine (12)	3.05(s), 4.06(s)	+0.58	-	+0.66	-
acetate (17)	1.93(s)	+0.62	+0.56	-	-
dimethylamine (15)	2.72(s)	-	-	+0.65	+0.58
trimethylamine-*N*-oxide (TMAO) (7)	3.27(s)	-	-	−0.71	−0.58
phenylacetylglycine (8)	3.68(s), 3.77(d), 7.43(t), 7.37(t)	+0.70	-	-	+0.66
taurine (14)	3.27(t), 3.43(t)	-	-	-	−0.58
formate (22)	8.47(s)	+0.64	-	-	-
pipecolic acid (24)	1.66(m), 1.88(m), 2.22(m), 3.04(m), 3.44(d), 3.61(dd)	-	-	+0.77	+0.78
unknown no. 1 (33)	1.20(d), 1.24(d), 3.67(m), 3.81(m), 4.05(m)	-	-	+0.85	+0.83
unknown no. 2 (34)	6.27(d), 6.30(d)	-	-	+0.94	+0.90

[a] The key is consistent with the metabolite numbers shown in Figure 2 (s = singlet, d = doublet, t = triplet, m = multiplet).

goodness of prediction (expressed as Q^2Y) values are given for each of the postinfection collection time points. Increasing strength of Q^2Y over time from day 2 to 4 postinfection corresponds to an increase in severity of infection, underscored by the declining PCV and the elevated parasitemia level. Although many of the changes associated with increasing severity were quantitative, the number of perturbed metabolites also altered and increased as a result of infection severity. This is a property of the failure of systemic homeostatic control that results in the enhanced use of minor pathways increasing the metabolic complexity (and entropy) of the system; analogous situations have been observed in drug metabolism studies.[25,26] Within the first 2 days postinfection, concentrations of urinary 2-oxoisocaproate, 2-oxoisovalerate, 3-methyl-2-oxovalerate, PAG, acetate and formate showed higher levels in the postinfected mice when compared to the preinfection time point. Additionally, PAG and dimethylamine were observed in urine obtained from *P. berghei*-infected mice at later time points, when compared to preinfection. Pipecolic acid was found to be one of the most discriminatory metabolites and was present only in the *P. berghei*-infected urine samples.

^{1}H NMR Spectroscopy of Mouse Plasma. Representative 1D ^{1}H NMR CPMG spectra of plasma samples obtained from mice 4−6 h before and 4 days after infection with *P. berghei* are shown in Figure 4. This experiment results in the attenuation of signals from fast relaxing protons from macromolecules and motionally constrained metabolites due to protein binding.[14] A number of low molecular weight metabolites, such as leucine, valine, lactate, alanine, acetate, pyruvate, citrate, creatine, choline, glycerophosphoryl choline (GPC), and glucose were identified in these plasma spectra as expected from previous studies.[27]

Multivariate Analysis of ^{1}H NMR CPMG Spectra of Plasma. O-PLS-DA models were constructed with one PLS component and one orthogonal component utilizing unit variance scaling applied to the ^{1}H NMR CPMG plasma spectra. The discrimination between mouse plasma samples obtained prior to and after *P. berghei* infection was evident, especially on days 3 and 4 postinfection (Figure 5). Q^2Y values 3 and 4 days postinfection were 0.76 and 0.64, respectively. The coefficient plots showed that the increase of the relative concentration of lactate became more significant from day 2 after infection with *P. berghei* onward, whereas glucose levels decreased at days 3 and 4 postinfection, together with decreased levels of creatine and GPC.

Table 3 summarizes the plasma metabolites that significantly contributed to separation between pre- and postinfection time points.

Discussion

Experimental infection of female NMRI mice with *P. berghei* induced a range of systemic metabolic perturbations in the urine and plasma of the host as early as 1 day postinfection, and these changes increased as the time to infection progressed. Although a satellite group of control mice were not given a sham injection of uninfected erythrocytes, the metabolic changes observed were not consistent with those associated with acute stress,[28,29] and hence, the findings of the current study are almost certainly associated with a direct metabolic response to the infection. A prominent finding in the analysis of plasma spectra was the marked depletion of glucose, and an increase in lactate and pyruvate on days 2−4 postinfection when compared with the preinfection time point. This finding conforms to previous observations that *Plasmodium*-parasitized erythrocytes utilize higher amounts of glucose, compared to normal erythrocytes.[30,31] Malaria parasites experience an intraerythrocytic asexual stage where the parasites require energy from the host, primarily *via* anaerobic glycolysis due to the lack of a functional tricarboxylic acid cycle in this stage.[32,33] Our results are consistent with the increased glycolysis-related enzyme activities in *P. berghei*-infected erythrocytes of mice reported already in the early 1980s.[30] With regard to anaerobic glycolysis, the accumulation of lactate may cause lactic acidosis, which can cause cardiac impairment and, indeed, has been identified as a significant biochemical predictor of death in patients with severe *P. falciparum* malaria.[34,35] In a recent study, Daily and colleagues have shown that significant changes occur in the gene expression profiles of malaria parasites obtained from the blood of humans carrying *P. falciparum*.[13] Three distinct transcriptional states of the

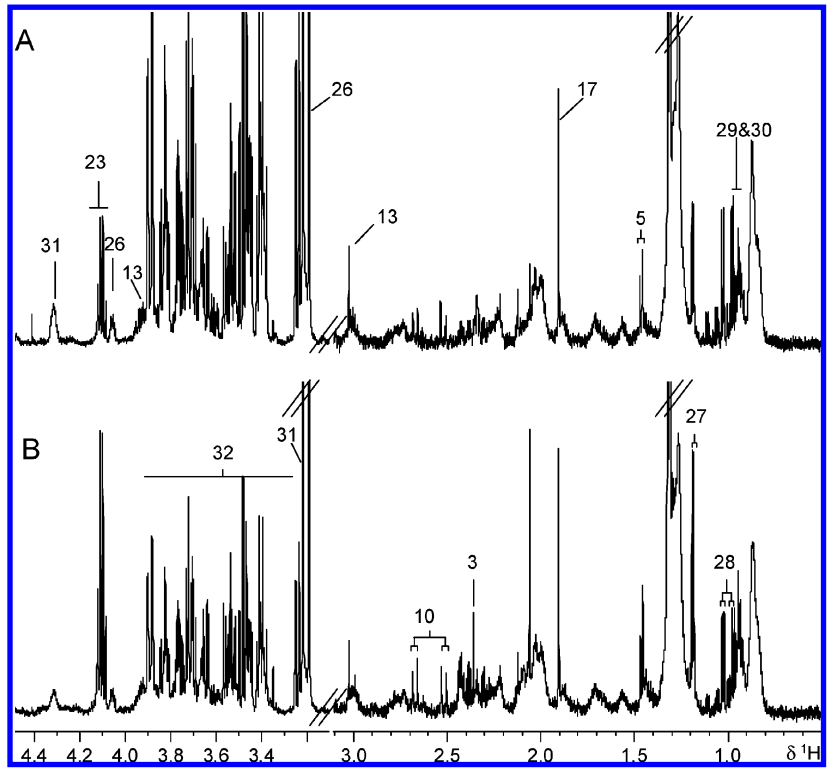

Figure 4. Representative 600 MHz ^{1}H NMR CPMG spectra of plasma samples collected from an uninfected mouse (A) and a mouse 4 days after a *P. berghei* infection (B). Key: 3, pyruvate; 5, alanine; 10, citrate; 13, creatine; 17, acetate; 23, lactate; 26, choline; 27, D-3-hydroxybutyrate; 28, valine; 29, leucine; 30, isoleucine; 31, glycerophosphoryl choline (GPC); 32, glucose.

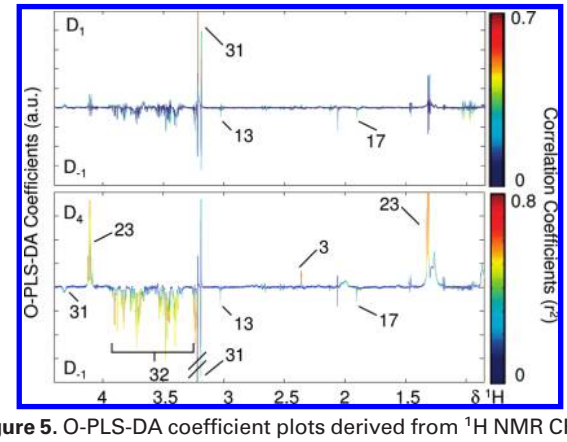

Figure 5. O-PLS-DA coefficient plots derived from ^{1}H NMR CPMG spectra of plasma obtained 4−6 h before infection (D_{-1}), and at days 1(D_1) and 4(D_4) postinfection revealing the metabolic fingerprint of a *P. berghei* infection and changes over time as the disease progressed. Resonances pointing upward indicated the increase of metabolic concentration in the infected mice. The model-derived Q^2Y values were 0.45 and 0.64 for days 1 and 4 postinfection, respectively.

parasite were reported, namely, (i) growth with glycolysis-provided energy, (ii) a starvation response of the parasite, and (iii) an environmental stress response. The observation of the first stage is consistent with our own metabolic findings obtained in female NMRI mice.

GPC in plasma was lower in *P. berghei*-infected mice at days 2−4 postinfection when compared to the preinfection time point. A report showing the presence of a high concentration of GPC in the adult filarial parasite *Brugia malayi* indicates that GPC is important for nutrient acquisition.[36] GPC also regulates phospholipid composition by inhibiting the enzyme lysolecithinase, and the disturbance of GPC may also suggest membrane abnormalities, as seen in the muscles of patients with Duchenne muscular dystrophy.[37] Another possibility is that the breakdown of GPC provides free choline to *Plasmodium*, since choline is taken up into parasite-infected erythrocyte, and phosphorylated by choline kinase.[38,39] Decreased levels of creatine were found in plasma of postinfected mice, which might be associated with the elevated concentration of plasma creatine phosphokinase (CPK). Indeed, increased levels of CPK is one of the biological indications of severe malaria.[40]

To our knowledge, we report—for the first time in a parasitic infection using a metabolic profiling strategy—elevated levels of pipecolic acid in urine of *P. berghei*-infected mice. Pipecolic acid is derived from either diet (e.g., dairy products, and fermented beverages) or catabolism of lysine by intestinal microbiota as depicted in Figure 6. In terms of the origin of pipecolic acid in mammalian urine, Fujita and colleagues found that it is mainly derived from lysine degradation rather than food intake.[41] In our study, all animals were fed on the same diet and maintained under the same environmental conditions, and hence, food intake seems unlikely to have contributed to the increased pipecolic acid, especially since there was no difference in the mean body weight of animals over the course of our experiment. It is interesting to note that elevated levels of pipecolic acid in plasma are recorded in patients with chronic liver disease, Dyggve-Melchior-Clausen syndrome, pyridoxine-dependent epilepsy, and Zellweger syndrome.[42−46] Pipecolic acid is known to act as a neuromodulator in the central nervous system, since it has been found to inhibit the initial gamma-aminobutyric acid (GABA; an inhibitory neurotransmitter) uptake, and to increase a high K^+-induced release of GABA.[47] The biological role of increased pipecolic acid in a *Plasmodium* infection is still unclear, since distur-

Table 3. Changes of Metabolites Observed in Plasma Obtained from Mice at Different Time Points after Infection with *P. berghei*, Compared with Preinfection Time Point

metabolite (key[a])	chemical shift (δ^1H)	importance of contribution at different time points postinfection			
		day 1 ($Q^2Y = 0.45$; $R^2X = 0.24$)	day 2 ($Q^2Y = 0.35$; $R^2X = 0.29$)	day 3 ($Q^2Y = 0.76$; $R^2X = 0.33$)	day 4 ($Q^2Y = 0.64$; $R^2X = 0.31$)
acetate (17)	1.91(s)	−0.66	−0.62	−0.55	−0.65
creatine (13)	3.03(s), 3.92(s)	−0.62	-	−0.69	−0.73
glycerophosphoryl choline (GPC) (31)	3.22(s), 3.67(m), 4.31(m)	+0.72	−0.61	−0.76	−0.80
lactate (23)	1.31(d), 4.11(q)	-	+0.73	+0.74	+0.71
pyruvate (3)	2.36(s)	-	+0.68	+0.77	+0.85
citrate (10)	2.53(d), 2.66(d)	-	-	+0.65	-
α-glucose	5.22(d)[b]	-	-	−0.72	−0.67

[a] The key is consistent with the metabolite numbers shown in Figure 4(s = singlet, d = doublet, q = quadruplet, m = multiplet). [b] α-Anomeric proton only reported as being representative of multiple α- and β-glucose resonances.

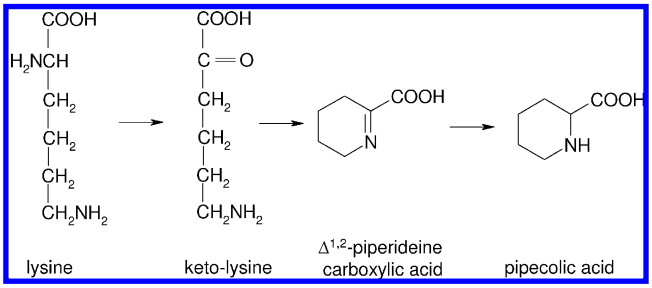

Figure 6. Biosynthesis of pipecolic acid from lysine.

bance of microbial community, liver dysfunction, and neurological damage are all known consequences of malaria infection.

Severe malaria is known to cause renal dysfunction.[48] The perturbation in levels of urinary dimethylamine and TMAO have been associated with renal cortex and papillary damage in methanol intoxication patients, and in proximal tubular toxins separately.[49,50] An increase of dimethylamine was found in the urine samples from mice at days 3 and 4 postinfection, which may be suggestive of renal dysfunction. However, histological examination of kidney removed from *P. berghei*-infected mice on termination of the experiment (after the final urine and plasma samples had been collected on day 4 postinfection) showed no clear evidence of pathological alterations in this organ (Figure 1). Importantly, altered excretion of dimethylamine and TMAO, which originate from choline, can also reflect a disturbance of the gut microbiota.[51] PAG, dimethylamine, and TMAO showed marked increases in urine samples obtained from postinfected mice. These metabolites are known to vary with changes in gut microbiota.[19] Therefore, the elevated excretion of PAG, dimethylamine, and TMAO observed in the current study may have resulted from the disturbance of microbial community by the *P. berghei* infection. One of the clinical symptoms of malaria is the high fever which could be responsible for the change of gut microbiota. However, little is known about the disturbance of the gut microbial ecosystem associated with malaria. Hence, further studies are warranted to investigate whether changes occur in gut microbiota over the course of a *P. berghei* infection.

In conclusion, we found changes in the urinary and plasma metabolic profiles of mice in response to a *P. berghei* infection, indicative of global changes in metabolic regulation and homeostasis. Hence, our findings underscore the extensive metabolic cross-talk between the host (i.e., NMRI mouse) and the parasite (i.e., *P. berghei* ANKA strain) *in vivo* and demonstrate the potential of a global metabolic profiling strategy based on ^{1}H NMR spectroscopy in conjunction with multivariate data analysis. Our strategy holds promise for extraction of biomarker information. Recently, the same NMR-based metabonomic approach has been employed to characterize the responses in female NMRI mice to a *Trypanosoma brucei brucei* infection.[21] Interestingly, an upregulation of glycolysis was found in both studies. Although both *Plasmodium* and *Trypanosoma* are protozoan parasites, the perturbation of observed amino acids in plasma were different with an increased level of creatine in *T. brucei brucei*, and a decreased level in *P. berghei*. Our analytical strategy presented here can be utilized for the development of novel, rapid, and noninvasive diagnostic methods. We conjecture that further development of ^{1}H NMR spectroscopy/mass spectrometry and pattern recognition-based techniques will provide the backbone for innovation, validation, and application of new diagnostic tools, drug targets and, eventually, vaccines against malaria and other parasitic diseases. One of the most useful applications of this technology could be the identification of asymptomatic cases, an important obstacle for contemporary malaria control efforts.[10]

Author Contributions. Y.W., B.H.S., S.W., E.H., and J.U. conceived and designed the experiment. S.W. and J.U. collected urine, blood and tissue samples from mice. S.D. analyzed and interpreted the histological data. J.V.L., Y.W., and J.S. performed the NMR experiments. J.V.L., Y.W., J.K.N., S.W., E.H., and J.U. analyzed the data. J.V.L, Y.W., J.K.N., B.H.S., M.T., S.W., E.H., and J.U. wrote the paper.

Acknowledgment. We thank J.C. Janse, Leiden University, for providing the GFP transfected *P. berghei* strain. We are grateful to J. Santo-Tomas and C. Snyder for their expert technical support with the host-parasite model. We also thank Dr. O. Cloarec and Dr. T. Ebbels for allowing us to use MATLAB script and NMRPROG to process NMR data. J.V.L., J.S., and J.U. receive financial support from the Swiss National Science Foundation (project no. PPOOB-102883, PPOOB-119129). J.V.L. is grateful to a Deputy Rector Award of Imperial College London. Y.W. acknowledges funding from Nestle. The authors have declared that no competing interests exist.

References

(1) Snow, R. W.; Guerra, C. A.; Noor, A. M.; Myint, H. Y.; Hay, S. I. The global distribution of clinical episodes of *Plasmodium falciparum* malaria. *Nature* **2005**, *434*, 214–217.

(2) Lopez, A. D.; Mathers, C. D.; Ezzati, M.; Jamison, D. T.; Murray, C. J. L. Global and regional burden of disease and risk factors, 2001: systematic analysis of population health data. *Lancet* **2006**, *367*, 1747–1757.

(3) Breman, J. G. The ears of the hippopotamus: manifestations, determinants, and estimates of the malaria burden. *Am. J. Trop. Med. Hyg.* **2001**, *64* (1−2 Suppl.), 1–11.
(4) Tuteja, R. Malaria—an overview. *FEBS J.* **2007**, *274*, 4670–4679.
(5) Rosenthal, P. J.; Lee, G. K.; Smith, R. E. Inhibition of a *Plasmodium vinckei* cysteine proteinase cures murine malaria. *J. Clin. Invest.* **1993**, *91*, 1052–1056.
(6) Stevenson, M. M.; Tam, M. F. Differential induction of helper T cell subsets during blood-stage *Plasmodium chabaudi* AS infection in resistant and susceptible mice. *Clin. Exp. Immunol.* **1993**, *92*, 77–83.
(7) Chen, M.; Theander, T. G.; Christensen, S. B.; Hviid, L.; Zhai, L.; Kharazmi, A. Licochalcone A, a new antimalarial agent, inhibits *in vitro* growth of the human malaria parasite *Plasmodium falciparum* and protects mice from *P. yoelii* infection. *Antimicrob. Agents Chemother.* **1994**, *38*, 1470–1475.
(8) Campanella, G. S. V.; Tager, A. M.; El Khoury, J. K.; Thomas, S. Y.; Abrazinski, T. A.; Manice, L. A.; Colvin, R. A.; Luster, A. D. Chemokine receptor CXCR3 and its ligands CXCL9 and CXCL10 are required for the development of murine cerebral malaria. *Proc. Natl. Acad. Sci. U.S.A.* **2008**, *105*, 4814–4819.
(9) Tanner, M.; de Savigny, D. Malaria eradication back on the table. *Bull. World Health Organ.* **2008**, *82*, 84.
(10) Coura, J. R.; Suárez-Mutis, M.; Ladeia-Andrade, S. A new challenge for malaria control in Brazil: asymptomatic *Plasmodium* infection—a review. *Mem. Inst. Oswaldo Cruz* **2006**, *101*, 229–237.
(11) Njama-Meya, D.; Kamya, M. R.; Dorsey, G. Asymptomatic parasitaemia as a risk factor for symptomatic malaria in a cohort of Ugandan children. *Trop. Med. Int. Health* **2004**, *9*, 862–868.
(12) Wongsrichanalai, C.; Barcus, M. J.; Muth, S.; Sutamihardja, A.; Wernsdorfer, W. H. A review of malaria diagnostic tools: microscopy and rapid diagnostic test (RDT). *Am. J. Trop. Med. Hyg.* **2007**, *77*, 119–127.
(13) Daily, J. P.; Scanfeld, D.; Pochet, N.; Le Roch, K.; Plouffe, D.; Kamal, M.; Sarr, O.; Mboup, S.; Ndir, O.; Wypij, D.; Levasseur, K.; Thomas, E.; Tamayo, P.; Dong, C.; Zhou, Y.; Lander, E. S.; Ndiaye, D.; Wirth, D.; Winzeler, E. A.; Mesirov, J. P.; Regev, A. Distinct physiological states of *Plasmodium falciparum* in malaria-infected patients. *Nature* **2007**, *450*, 1091–1095.
(14) Nicholson, J. K.; Wilson, I. D. High-resolution proton magnetic-resonance spectroscopy of biological fluids. *Prog. NMR Spectrosc.* **1989**, *21*, 449–501.
(15) Nicholson, J. K.; Lindon, J. C.; Holmes, E. 'Metabonomics': understanding the metabolic responses of living systems to pathophysiological stimuli via multivariate statistical analysis of biological NMR spectroscopic data. *Xenobiotica* **1999**, *29*, 1181–1189.
(16) Nicholson, J. K.; Connelly, J.; Lindon, J. C.; Holmes, E. Metabonomics: a platform for studying drug toxicity and gene function. *Nat. Rev. Drug Discovery* **2002**, *1*, 153–161.
(17) Martin, F. P. J.; Dumas, M. E.; Wang, Y. L.; Legido-Quigley, C.; Yap, I. K. S.; Tang, H.; Zirah, S.; Murphy, G. M.; Cloarec, O.; Lindon, J. C.; Sprenger, N.; Fay, L. B.; Kochhar, S.; van Bladeren, P.; Holmes, E.; Nicholson, J. K. A top-down systems biology view of microbiome-mammalian metabolic interactions in a mouse model. *Mol. Syst. Biol.* **2007**, *3*, 112.
(18) Martin, F. P. J.; Wang, Y. L.; Sprenger, N.; Yap, I. K. S.; Lundstedt, T.; Lek, P.; Rezzi, S.; Ramadan, Z.; van Bladeren, P.; Fay, L. B.; Kochhar, S.; Lindon, J. C.; Holmes, E.; Nicholson, J. K. Probiotic modulation of symbiotic gut microbial-host metabolic interactions in a humanized microbiome mouse model. *Mol. Syst. Biol.* **2008**, *4*, 157.
(19) Wang, Y. L.; Holmes, E.; Nicholson, J. K.; Cloarec, O.; Chollet, J.; Tanner, M.; Singer, B. H.; Utzinger, J. Metabonomic investigations in mice infected with *Schistosoma mansoni*: an approach for biomarker identification. *Proc. Natl. Acad. Sci. U.S.A.* **2004**, *101*, 12676–12681.
(20) Wang, Y. L.; Utzinger, J.; Xiao, S. H.; Xue, J.; Nicholson, J. K.; Tanner, M.; Singer, B. H.; Holmes, E. System level metabolic effects of a *Schistosoma japonicum* infection in the Syrian hamster. *Mol. Biochem. Parasitol.* **2006**, *146*, 1–9.
(21) Wang, Y. L.; Utzinger, J.; Saric, J.; Li, V. L.; Burckhardt, J.; Dirnhofer, S.; Nicholson, J. K.; Singer, B. H.; Brun, R.; Holmes, E. Global metabolic responses of mice to *Trypanosoma brucei brucei* infection. *Proc. Natl. Acad. Sci. U.S.A.* **2008**, *105*, 6127–6132.
(22) Franke-Fayard, B.; Trueman, H.; Ramesar, J.; Mendoza, J.; van der Keur, M.; van der Linden, R.; Sinden, R. E.; Waters, A. P.; Janse, C. J. A *Plasmodium berghei* reference line that constitutively expresses GFP at a high level throughout the complete life cycle. *Mol. Biochem. Parasitol.* **2004**, *137*, 23–33.
(23) Vennerstrom, J. L.; Arbe-Barnes, S.; Brun, R.; Charman, S. A.; Chiu, F. C.; Chollet, J.; Dong, Y.; Dorn, A.; Hunziker, D.; Matile, H.; McIntosh, K.; Padmanilayam, M.; Santo Tomas, J.; Scheurer, C.; Scorneaux, B.; Tang, Y.; Urwyler, H.; Wittlin, S.; Charman, W. N. Identification of an antimalarial synthetic trioxolane drug development candidate. *Nature* **2004**, *430*, 900–904.
(24) Trygg, J.; Wold, S. Orthogonal projections to latent structures (O-PLS). *J. Chemom.* **2002**, *16*, 119–128.
(25) Wilson, I. D.; Nicholson, J. K. Topics in xenobiochemistry: do metabolic pathways exist for xenobiotics? The micro-metabolism hypothesis. *Xenobiotica* **2003**, *33*, 887–901.
(26) Nicholson, J. K.; Holmes, E.; Wilson, I. D. Gut microorganisms, mammalian metabolism and personalized health care. *Nat. Rev. Microbiol.* **2005**, *3*, 431–438.
(27) Nicholson, J. K.; Foxall, P. J. D.; Spraul, M.; Farrant, R. D.; Lindon, J. C. 750 MHz ^{1}H and ^{1}H-^{13}C NMR spectroscopy of human blood plasma. *Anal. Chem.* **1995**, *67*, 793–811.
(28) Wang, Y. L.; Lawler, D.; Larson, B.; Ramadan, Z.; Kochhar, S.; Holmes, E.; Nicholson, J. K. Metabonomic investigations of aging and caloric restriction in a life-long dog study. *J. Proteome Res.* **2007**, *6*, 1846–1854.
(29) Teague, C. R.; Dhabhar, F. S.; Barton, R. H.; Beckwith-Hall, B.; Powell, J.; Cobain, M.; Singer, B.; McEwen, B. S.; Lindon, J. C.; Nicholson, J. K.; Holmes, E. Metabonomic studies on the physiological effects of acute and chronic psychological stress in Sprague-Dawley rats. *J. Proteome Res.* **2007**, *6*, 2080–2093.
(30) Kruckeberg, W. C.; Sander, B. J.; Sullivan, D. C. *Plasmodium berghei*: glycolytic enzymes of the infected mouse erythrocyte. *Exp. Parasitol.* **1981**, *51*, 438–443.
(31) Roth, E. F. J.; Calvin, M. C.; Max-Audit, I.; Rosa, J.; Rosa, R. The enzymes of the glycolytic pathway in erythrocytes infected with *Plasmodium falciparum* malaria parasites. *Blood* **1988**, *72*, 1922–1925.
(32) Lang-Unnasch, N.; Murphy, A. D. Metabolic changes of the malaria parasite during the transition from the human to the mosquito host. *Annu. Rev. Microbiol.* **1998**, *52*, 561–590.
(33) Mehta, M.; Sonawat, H. M.; Sharma, S. Malaria parasite-infected erythrocytes inhibit glucose utilization in uninfected red cells. *FEBS Lett.* **2005**, *579*, 6151–6158.
(34) Agbenyega, T.; Angus, B. J.; Bedu-Addo, G.; Baffoe-Bonnie, B.; Guyton, T.; Stacpoole, P. W.; Krishna, S. Glucose and lactate kinetics in children with severe malaria. *J. Clin. Endocrinol. Metab.* **2000**, *85*, 1569–1576.
(35) Ehrhardt, S.; Mockenhaupt, F. P.; Anemana, S. D.; Otchwemah, R. N.; Wichmann, D.; Cramer, J. P.; Bienzle, U.; Burchard, G. D.; Brattig, N. W. High levels of circulating cardiac proteins indicate cardiac impairment in African children with severe *Plasmodium falciparum* malaria. *Microbes Infect.* **2005**, *7*, 1204–1210.
(36) Shukla-Dave, A.; Degaonkar, M.; Roy, R.; Murthy, P. K.; Murthy, P. S.; Raghunathan, P.; Chatterjee, R. K. Metabolite mapping of human filarial parasite *Brugia malayi* with nuclear magnetic resonance. *Magn. Reson. Imaging* **1999**, *17*, 1503–1509.
(37) Sharma, U.; Atri, S.; Sharma, M. C.; Sarkar, C.; Jagannathan, N. R. Skeletal muscle metabolism in Duchenne muscular dystrophy (DMD): an *in-vitro* proton NMR spectroscopy study. *Magn. Reson. Imaging* **2003**, *21*, 145–153.
(38) Ancelin, M. L.; Vial, H. J. Choline kinase activity in *Plasmodium*-infected erythrocytes: characterization and utilization as a parasite-specific marker in malarial fractionation studies. *Biochim. Biophys. Acta* **1986**, *875*, 52–58.
(39) Lehane, A. M.; Saliba, K. J.; Allen, R. J. W.; Kirk, K. Choline uptake into the malaria parasite is energized by the membrane potential. *Biochem. Biophys. Res. Commun.* **2004**, *320*, 311–317.
(40) Saïssy, J. M.; Vitris, M.; Diatta, B.; Kempf, J.; Adam, F.; Sarthou, J. L. Severe malaria in African adults living in a seasonal endemic area. *Intensive Care Med.* **1994**, *20*, 437–441.
(41) Fujita, T.; Hada, T.; Higashino, K. Origin of D- and L-pipecolic acid in human physiological fluids: a study of the catabolic mechanism to pipecolic acid using the lysine loading test. *Clin. Chim. Acta* **1999**, *287*, 145–156.
(42) Danks, D. M.; Tippett, P.; Adams, C.; Campbell, P. Cerebro-hepato-renal syndrome of Zellweger. A report of eight cases with comments upon the incidence, the liver lesion, and a fault in pipecolic acid metabolism. *J. Pediatr.* **1975**, *86*, 382–387.
(43) Kawasaki, H.; Hori, T.; Nakajima, M.; Takeshita, K. Plasma levels of pipecolic acid in patients with chronic liver disease. *Hepatology* **1988**, *8*, 286–289.
(44) Roesel, R. A.; Carroll, J. E.; Rizzo, W. B.; van der Zalm, T.; Hahn, D. A. Dyggve-Melchior-Clausen syndrome with increased pipecolic acid in plasma and urine. *J. Inherit. Metab. Dis.* **1991**, *14*, 876–880.

(45) Matsuda, Y.; Fujita, T.; Hada, T.; Higashino, K. Comparative study on the correlation of plasma gamma-aminobutyric acid and pipecolic acid with liver function in patients with liver cirrhosis. *Hepatol. Res.* **2000**, *18*, 132–140.
(46) Plecko, B.; Stockler-Ipsiroglu, S.; Paschke, E.; Erwa, W.; Struys, E. A.; Jakobs, C. Pipecolic acid elevation in plasma and cerebrospinal fluid of two patients with pyridoxine-dependent epilepsy. *Ann. Neurol.* **2000**, *48*, 121–125.
(47) Nomura, Y.; Okuma, Y.; Segawa, T.; Schmidt-Glenewinkel, T.; Giacobini, E. Comparison of synaptosomal and glial uptake of pipecolic acid and GABA in rat brain. *Neurochem. Res.* **1981**, *6*, 391–400.
(48) Day, N. P. J.; Hien, T. T.; Schollaardt, T.; Loc, P. P.; Chuong, L. V.; Chau, T. T. H.; Mai, N. T. H.; Phu, N. H.; Sinh, D. X.; White, N. J.; Ho, M. The prognostic and pathophysiologic role of pro- and antiinflammatory cytokines in severe malaria. *J. Infect. Dis.* **1999**, *180*, 1288–1297.
(49) Gartland, K. P. R.; Bonner, F. W.; Nicholson, J. K. Investigations into the biochemical effects of region-specific nephrotoxins. *Mol. Pharmacol.* **1989**, *35*, 242–250.
(50) Janus, T.; Borowiak, K. S.; Pabisiak, K.; Machoy-Mokrzynska, A.; Swiniarski, A.; Rozwadowski, Z. ^{1}H nuclear magnetic resonance spectroscopic investigation of urine for diagnostic and clinical assessment of methanol intoxication. *Basic Clin. Pharmacol. Toxicol.* **2005**, *97*, 257–260.
(51) Dumas, M. E.; Barton, R. H.; Toye, A.; Cloarec, O.; Blancher, C.; Rothwell, A.; Fearnside, J.; Tatoud, R.; Blanc, V.; Lindon, J. C.; Mitchell, S. C.; Holmes, E.; McCarthy, M. I.; Scott, J.; Gauguier, D.; Nicholson, J. K. Metabolic profiling reveals a contribution of gut microbiota to fatty liver phenotype in insulin-resistant mice. *Proc. Natl. Acad. Sci. U.S.A.* **2006**, *103*, 12511–12516.

PR800209D